2012 International Conference on Environmental, Biomedical and Biotechnology
IPCBEE vol.41 (2012) © (2012) IACSIT Press, Singapore

Active Manipulation of ECM Microscale Stiffness

Sahan C. B. Herath[1,2], Peter C. Y. Chen[1,2,+], Du Yue[1,2], Shi Hui[2], Dong-an Wang[3], Qingguo Wang[5] and Harry Asada[2,5]

[1] Department of Mechanical Engineering, National University of Singapore, Singapore
[2] BioSyM, Singapore-MIT Alliance for Research and Technology Program, Singapore
[3] Division of Bioengineering Nanyang Technological University, Singapore
[4] Department of Electrical and Computer Engineering, National University of Singapore, Singapore
[5] Department of Mechanical Engineering, Massachusetts Institute of Technology, USA

Abstract. This paper describes an approach to manipulate the stiffness of extracellular matrix, and reports the experimental results obtained from the atomic force microscopy to demonstrate the effectiveness of this proposed approach. The experimental results demonstrate that, by embedding magnetic beads in an ECM sample through bioconjugation between the streptavidin-coated beads and the collagen fibers, the stiffness of the ECM can be actively manipulated by the application of an external magnetic field. These results demonstrate the possibility of creating desired stiffness gradients in the ECM *in* to influence cell behavior.

Keywords: Stiffness, Extracellular matrix, Manipulation, Magnetic field, Beads, AFM

1. Introduction

The stiffness of the ECM (an insoluble cue) is known to influence many types of cellular behavior [1, 3]. It regulates the degree of cell-matrix adhesion, the size of the focal adhesion, as well as the stiffness and tension developed by the cell itself [2, 4]. Motility and cell alignment are associated with ECM stiffness, manifested in the tendency of cells to migrate from soft to stiff environment [5]. Although the mechanisms of many of these effects are still unknown, it is clear that the mechanical properties of the ECM influence protein expression [6].

A number of methods have been proposed in the literature for changing the stiffness of collagen for the purpose of observing *in vitro* cell behavior in an ECM sample. One involves changing collagen concentration. Helary *et al* showed the relationship between the collagen gel stiffness and collagen concentration [8]. Another method involves varying the pH value in a sample, since solution acidity during fibrillogenesis affects collagen stiffness [9]. Changing the temperature of an ECM sample can also lead to change in its stiffness [10]. These currently known methods mainly rely on manipulating soluble cues.

Manipulating the stiffness of ECM by mechanical means offers an alternative. In our previous work [7], we proposed an approach for active uniaxial manipulation of the stiffness of ECM samples. This approach works by embedding magnetic beads in an ECM through bio-conjugation between the streptavidin-coated beads and the collagen fibers, then applying an external magnetic field to exert forces on the beads in order to manipulate the stiffness of the ECM. In [7], the changes in the apparent stiffness of the ECM samples were observed at macroscale, where the ECM was treated as a lumped model whose stiffness was evaluated through stretch testing. The questions of how and to what extent the beads (when under the influence of the external magnetic field) affect the stiffness of the ECM locally at *microscale* remain to be explored.

+ Corresponding author. Tel.: (+65) 6516 8837.
E-mail address: mpechenp@nus.edu.sg

In this paper, we describe the design of an experiment to investigate the local stiffness of ECM samples using an Atomic Force Microscope (AFM). We then present an analytical model describing the change in the stiffness of a bead-embedded ECM sample due to the influence of an external magnetic field. Lastly, we report experimental results demonstrating the effectiveness of this approach for active manipulation of ECM stiffness and the validity of the analytical model.

2. Experiment Design and Procedure

We embedded superparamagnetic particles in ECM samples (via bioconjugation between the beads and the ECM fibers) and then apply an external magnetic field to actively manipulate the ECM stiffness. The beads are attached to the ECM fibers by bioconjugation. When the AFM indents at a location in the ECM near a bead, applying an external magnetic field produces a force on the beads. The forces acting on the beads are transmitted through the fibers to produce in the ECM a resistance to the indentation of the AFM. The change in the Young's modulus of the ECM sample, when switching on or off the magnetic field, is determined by the AFM. We investigated four scenarios listed in Table 1.

Table 1: Scenarios in Experiment

No.	***1***	***2***	***3***	***4***
Bioconjugation	Yes	Yes	No	No
Magnetic field	Off	On	Off	On

For Scenarios 1 and 2, we used beads coated with streptavidin since streptavidin will affix to collagen-rich areas [12, 13]. For Scenarios 3 and 4, we need to embed beads in the ECM such that there is no binding between the beads and the collagen fibers. The collagen was prepared according to the recipes listed in Table 2. A holder was designed to contain the magnet and the collagen in close proximity to each other. A 4 mm^3 cube, grade N50 Neodymium Iron Boron permanent magnet, procured from Liftonmagnet, was to be housed in this holder. Fig. 1 shows a solid-model image of the holder and the actual item fabricated by using an Eden 350 3D printer, and a JPK NanoWizard II AFM module, incorporated with a tip-scanning concept for long-time position stability was used in conjunction with a 4-μm-diameter microsphere as the probe.

Table 2: Recipes for Collagen Preparation

Components	***Without magnetic beads***	***With magnetic beads (Streptavidin coated)***	***With magnetic beads (PEG coated)***
Collagen (4.62 mg/mL)	0.216 mL	0.216 mL	0.216 mL
Water	0.137 mL	0.131 mL	0.131 mL
PBS (10x)	0.040 mL	0.040 mL	0.040 mL
NaOH (0.5 N)	0.007 mL	0.007 mL	0.007 mL
Beads (5 mg/mL)	0 mL	0.006 mL	0.006 mL
Total	0.400 mL	0.400 mL	0.400 mL

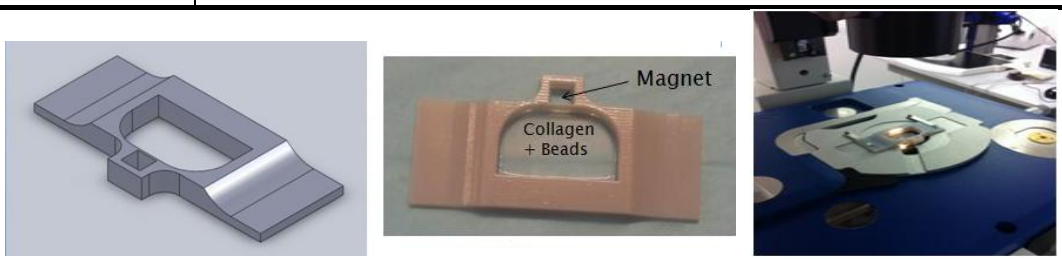

Fig. 1: Solid model and actual holder.

Under the conditions that the sample are considered as an isotropic and linear elastic solid occupying an infinitely extending half, that the indenter is non-deformable, and that there are no additional interactions between indenter and the sample, the Young modulus (E) of the sample can be fitted and calculated using the Hertz model, which has the form [11]:

$$F = \frac{4ER^{1/2}}{3(1-\nu^2)}\delta^{3/2}\left[1 - \frac{2\alpha_0}{\pi}\chi + \frac{4\alpha_0^2}{\pi^2}\chi^2 - \frac{8}{\pi^3}\left(\alpha_0^3 + \frac{4\pi^2}{15}\beta_0\right)\chi^3 + \frac{16\alpha_0}{\pi^4}\left(\alpha_0^3 + \frac{3\pi^2}{5}\beta_0\right)\chi^4\right] \quad (1)$$

with the Poisson's ratio set at $v = 0.5$ for soft biological samples, $\alpha_0 = -1.2876 - 1.4678v + 1.3442v^2/(1 - v)$ and $\beta_0 = 0.6387 - 1.0277v + 1.5164v^2/(1 - v)$, where $x = \sqrt{R\delta}\ /\ h$, δ is the sample indentation, h is the sample height, R is the radius of the indentation sphere, and E is the Young's modulus of the sample, as indicated in Fig. 2.

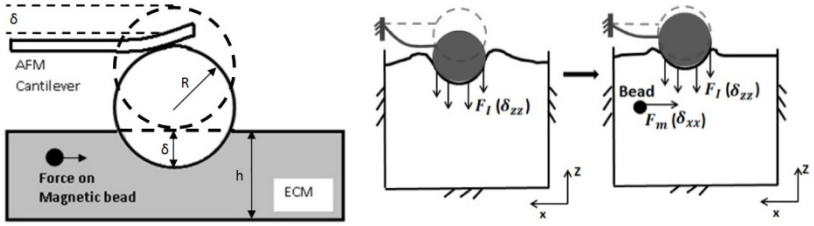

Fig. 2: Schematic of the AFM spherical probe tip during the indentation experiment.

When compared to the depth of indentation which is to be limited to a maximum of 5 μm in this experiment, the sample height of $h = 800$ μm can be considered as infinitely large. With $\chi \to 0$, the force-indentation relationships, as shown in Equation (1), reduce to $F = \lambda\delta^{3/2}$. In particular, for an AFM with a spherical tip, $\lambda = 4E\ R^{1/2} / (3(1 - v^2))$. Therefore, $F = 4E\ R^{1/2}\ \delta^{3/2} / (3(1 - v^2))$. By measuring F and δ experimentally, we can estimate E for a given ECM sample.

For each sample associated with a scenario specified in Table 1, a set of force and indentation depth measurements were obtained along Line 1 in the y-direction as shown in Fig. 3. Another set of measurements will be taken along Line 2, which is separated from Line 1 in the x-direction by about 50 μ m. Two reference points were chosen along each line and fifteen to twenty measurements were taken at random positions. Fig. 3 illustrates the details of the indentations.

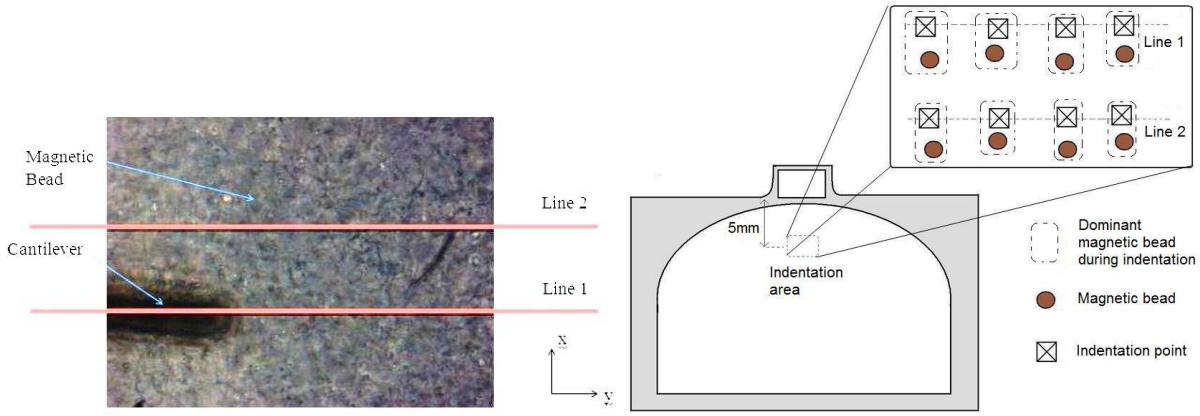

Fig. 3: Illustration of indentation areas and bead locations.

3. Analysis of Change in ECM Stiffness

The magnetic field equation along the x-axis (as is indicated in Fig. 3) for a cuboid permanent magnet is given by [15],

$$B_x(x) = \frac{B_r}{\pi}\left[\tan^{-1}\left(\frac{ab}{2x\sqrt{4x^2+a^2+b^2}}\right) - \tan^{-1}\left(\frac{ab}{2(c+x)\sqrt{4(c+x)^2+a^2+b^2}}\right)\right] \quad (3)$$

where $a = b = c = 4$ mm are the height, width and thickness of the permanent magnet, respectively. With $B_r = 1.5$ T, a bead approximately 5 mm away from the magnet will experience a magnetic field of $B = 0.05$ T. According to the magnetization curve (provided by Bangs Laboratory, Inc.), such a bead has an induced auxiliary magnetic field of $H = 40$ emu/g. The force experienced by a bead is [14]: $F = \nabla(m \bullet B)$, where the magnetic moment can be obtained as $m = \rho \bullet H \bullet V$, with $\rho = 5.24$ kg/m^3 is the density of iron oxide, and V the volume of a bead with a radius of 1 μm. A numerical simulation for the case of a bead located at a distance of $x = 5$ mm away from the magnet shows that the force acting on the bead is approximately 16 pN.

With the AFM indenting the region of the sample near a bead in the $-z$ direction and the magnetic force exerting on the bead in the $-x$ direction, as is illustrated in Fig. 3, the strain generated by the stress tensor of the indentation force is $\varepsilon_{zz} = (1/E)\ [-\nu\ -\nu\ 1]\ [\sigma_{xx}\ \sigma_{yy}\ \sigma_{zz}]^T$. For this case the shear stress can be ignored. When the magnetic field is absent, we have $\sigma_{xx} = \sigma_{yy} = 0$. Using the contact model of a sphere and a half space, σ_{zz} can be expressed as $\sigma_{zz} = -F_I / \pi R d$, where F_I is the force applied by the AFM. Consequently, $\varepsilon'_{zz} = -F_I / \pi E R d$. When present, the magnetic field contributes to the stress tensor in the x direction so that $\sigma_{xx} = -F_m / \pi R_b^2$, where F_m is the magnetic force exerted on bead, and R_b is the radius of bead. Thus, the strain in the z direction is reduced to $\varepsilon'_{zz} = (\sigma_{zz} - \nu\sigma_{xx})/E = (-F_I / \pi R d + \nu F_m / \pi R_b^2)/E$. Therefore,

$$E'_{zz} = -F_I/\pi R d\varepsilon'_{zz} = -EF_I R_b^2/\left(\nu F_m R d - F_I R_b^2\right) \tag{4}$$

4. Results and Discussion

Fig. 4 shows one pair of results (for samples embedded with streptavidin-coated beads and with PEG coated beads) that were obtained in the absence (Fig. 4a) and the presence (Fig. 4b) of the magnetic field. The average readings of the Young's modulus for Line 1 and Line 2 were calculated and the line that gave the least standard deviation was chosen for comparison. The average stiffness associated with the four scenarios are shown in Table 3. Using Equation (4) and under the condition that there is a bead closest to the indentation site that generates the dominant resistant to the indentation (as illustrated in Fig. 3), the new Young's modulus can be calculated (by setting F_m = 16 pN and using the Young's modulus for the case of no magnetic field) to be 41.58 Pa. This represents an (analytically predicted) 13.63% increase in the Young's modulus of the sample when the magnetic field was applied, and is comparable with the experimental result (of a 16.23% increase) as shown in Table 3.

From Table 3, it can also be seen that the Young's modulus of the sample embedded with PEG-coated beads decreased by 9% upon the application of the magnetic field. This decrease can be explained by the fact that the PEG-coated beads had no strong attachment to the ECM fibers. When the magnetic force was applied, the individual beads were pulled and dislocated slightly from their original surrounding. This created space around a bead for it to move around easily. When the sample was indented by the AFM, there was then less resistance (due to the beads) against the movement of the AFM tip, resulting in the observed reduction in the value of the Young's modulus.

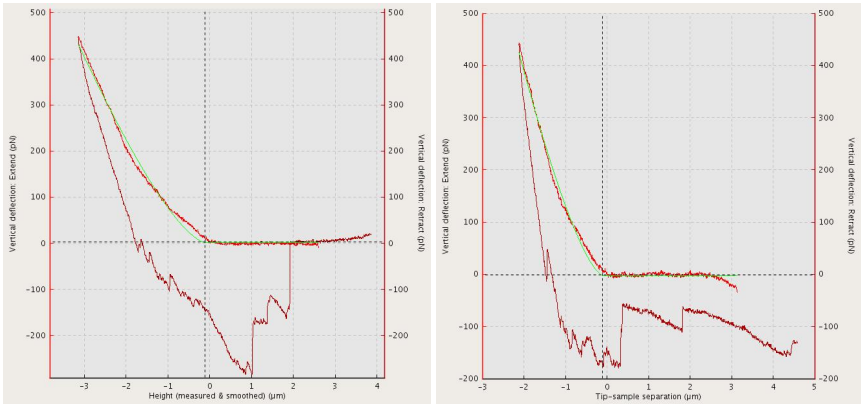

(a) AFM result without magnetic field (b) AFM result with magnetic field

Fig. 4: AFM indentation results.

Table 3: Summary of results

Sample	*Magnetic field [Stiffness (Pa)]*	*Percentage change (%)*
ECM with beads embedded but no binding	off [14.96], on [13.59]	-9.12
ECM with beads embedded with binding	off [36.59], on [42.53]	16.23

5. Conclusion

We have presented the design of an experiment to investigate the local stiffness of ECM samples using an Atomic Force Microscope, and have developed an analytical model to predict the change in the stiffness of a bead-embedded ECM sample due to the influence of an external magnetic field. We have also reported experimental results demonstrating the effectiveness of this approach for active manipulation of ECM stiffness and the validity of the analytical model. Our experimental results have demonstrated that the binding between the embedded beads and the collagen fibers plays a significant role in affecting the overall stiffness of ECM. This is due to the fact that beads attached to the fibers via bioconjugation create substantial additional resistance to deformation in the fibers when an external magnetic field is applied. These results demonstrate the possibility of creating desired stiffness gradients in an *in vitro* extracellular matrix to influence cell behavior.

6. Acknowledgements

The authors would like to thank the BioSystems and Micromechanics Interdisciplinary Research Group (under the Singapore-MIT Alliance for Research and Technology Program) for financial support. The first author would like to acknowledge the financial support provided by the National University of Singapore (NUS). The third author would like to acknowledge the financial support provided by the China Scholarship Council and by the Department of Mechanical Engineering at NUS.

7. References

[1] J. P. Jr Robert and Yu-Li Wang. Cell locomotion and focal adhesions are regulated by substrate flexibility. *Proc. Natl. Acad. Sci. U S A*. 1997, **94** (25): 13661-13665.

[2] R.G. Wells. The role of matrix stiffness in regulating cell behavior. *Hepatology*. 2008, **47**(4): 1394-1400.

[3] R. K. Assoian and E. A. Klein. Growth control by intracellular tension and extracellular stiffness. *Trends Cell Biol.* 2008, **18** (7): 347-352.

[4] J. E. Adam, S. Sen, H. L. Sweeney and D. E. Discher. Matrix elasticity directs stem cell lineage specification. *Cell*. 2006, **126**, 677-689.

[5] B. Harland, S. Walcott and S. X. Sun. Adhesion dynamics and durotaxis in migrating cells. *Phys. Biol.* 2011, **8** (1): 015011.

[6] M. H. Zaman, L. M. Trapani, A. L. Sieminski, D. Mackerllar, H. Gong, R. D. Kamm, A. Wells, D. A. Lauffenburger and P. Matsudaira. Migration of tumor cells in 3D matrices is governed by matrix stiffness along with cell-matrix adhesion and proteolysis. *PNAS*. 2006, **103** (29), 10889-10894.

[7] C. Y. Chen Peter, S. C. Herath, Dong-An Wang, K. Su, K. Liao and H. Asada. Active manipulation of uniaxial ECM stiffness by magnetic anchoring of bio-conjugated beads. *ASME Summer Bioengineering Conference*. Pennsylvania. 2011, pp. 1-14.

[8] D. M. Knapp, V. H. Barocas and A. G. Moon. Rheology of reconstituted type I collagen gel in confined compression. *J. Rheol.* 1997, **4**1(5), 971- 993.

[9] C. Helary, I. Bataille, A. Abed, C. Illoul, A. Anglo, L. Louedec, D. Letourneur , A. Meddahi-Pell, M. M. Giraud-Guille. Concentrated collagen hydrogels as dermal substitutes. *Biomaterials*. 2010, **31** (3), 481-490.

[10] D. L. Christiansen, E. K. Huang and F. H. Silver. Assembly of type I collagen: fusion of fibril subunits and the influence of fibril diameter on mechanical properties. *Matrix Biol.* 2010, **19**(5), 409-420.

[11] C. B. Raub, V. Suresh, T. Krasieva, J. Lyubovitsky, J. D. Mih, A. J. Putnam, B. J. Tromberg, S. C. George. Noninvasive assessment of collagen gel microstructure and mechanics using multiphoton microscopy. *Biophys. J.* 2007, **92**, 2212-2222.

[12] K. D. Emilios, H. Ferenc, M. Julia, K. Bechara and S. C. Richard. Determination of elastic moduli of thin layers of soft material using the atomic force microscope. *Biophys. J.* 2002, **82** (5), 2798-2810.

[13] S. Freitag, I. Le Trong, L. Klumb, P. S. Stayton and R. E. Stenkamp. Structural studies of the Streptavidin binding loop. *Protein Sci.* 1997, **6** (6), 1157-1166.

[14] L. Harvey, A. K. Chris, B. Arnold, K. Monty, M. Paul and P. S. Matthew. *Molecular Cell Biology*. W H Freeman, 2008.

[15] P. Kollmannsberger and B. Fabry. High-force magnetic tweezers with force feedback for biological applications *Rev. Sci. Instrum.*. 2007, **78**, 114301.

[16] J. Lipfert, X. Hao, and N. H. Dekker. Quantitative Modeling and Optimization of Magnetic Tweezers. *Biophys. J.* 2009, **96**, 5040-5049.